

**Title: High Parasite Diversity Accelerates Host Adaptation And Diversification**

**Authors:** A. Betts<sup>1\*</sup>, C. Gray<sup>2</sup>, M. Zelek<sup>1</sup>, R.C. MacLean<sup>1+</sup>, K.C. King<sup>1\*+</sup>.

**Affiliations:**

<sup>1</sup>Department of Zoology, University of Oxford, South Parks Road, Oxford OX1 3PS, UK

<sup>2</sup>Department of Life Sciences, Imperial College London, Silwood Park Campus, Ascot, SL5 7PY, UK

\*Corresponding authors. E-mail: [Alex.Betts@evobio.eu](mailto:Alex.Betts@evobio.eu), [Kayla.King@zoo.ox.ac.uk](mailto:Kayla.King@zoo.ox.ac.uk)

<sup>+</sup> contributed equally

**One Sentence Summary:** Increasing parasite diversity accelerates coevolutionary arms races and leads to greater generalist host resistance.

**Abstract:** Host-parasite species pairs can coevolve, but the impacts of diverse parasite communities on coevolution are unclear. By using experimental coevolution of a host bacterium and viral parasites, we revealed that diverse parasite communities accelerated host evolution and altered coevolutionary dynamics, resulting in enhanced host resistance and decreased parasite infectivity. Increases in parasite diversity drove shifts in the mode of selection from fluctuating (Red Queen dynamics) to predominately directional (Arms Race dynamics). The latter was characterized by selective sweeps of generalist resistance mutations in LPS biosynthesis genes, which caused faster molecular evolution within host populations and greater genetic divergence among populations. These results suggest that parasite communities can have profound effects on the rate and mechanism of host-parasite coevolution.

**Main Text:**

Coevolution between hosts and parasites is hypothesized as central to numerous biological phenomena, from rapid evolutionary change (1) to the maintenance of diversity (2) and sexual reproduction (3, 4). Host-parasite coevolution is traditionally investigated in a pairwise framework where a single parasite species infects one host species (5). However, in nature, these pairwise relationships rarely exist in isolation (6, 7): hosts are often under attack by multiple parasite species (8), and parasites must compete for hosts (9–12). Host-parasite coevolution thus operates within a network of species interactions (13). It nevertheless remains unknown whether and how diverse parasite communities can shape coevolutionary patterns and processes.

Coevolution with highly diverse parasite communities should impose stronger selection for host resistance if this diversity yields more infections and higher mortality than single parasites. This is an outcome that could ultimately drive faster host evolution and increased divergence among host populations. To test these predictions, we applied an experimental coevolution approach to an *in vitro* bacteria-phage system. We exposed the host bacterium, *Pseudomonas aeruginosa*, to communities of one to five lytic viral parasites (bacteriophages PEV2, LUZ19, LUZ7, 14-1 and LMA2) that are obligate lethal parasites. These parasites infect their hosts by each attaching to one of three specific cell surface receptors (lipopolysaccharides (LPS), Ton-B dependent receptors or Type IV pili) and hosts typically evolve resistance by modifying or deleting these attachment sites (14). Parasites, in turn, can evolve reciprocal adaptations to circumvent host resistance (15). Specifically, we experimentally coevolved host populations independently in cell culture tubes with replicates of a five-parasite community (High Diversity, N=30) alongside every possible pairwise parasite combination (Medium, N=30) and a single parasite treatment with replicates of each

in monoculture (Low, N=30) alongside a parasite-free control (N=30). We tested for effects on the tempo and mode of host-parasite coevolution, conducting phenotypic assays of host resistance and parasite infectivity, as well as by using deep sequencing to measure changes in the genomic composition of host and parasite populations through time. Because we are able to experimentally manipulate parasite diversity, our work differs from the approaches used to investigate coevolution in natural communities, where diversity is not controlled exogenously (16, 17).

As with predators and prey, parasite densities are expected to track host densities producing time-lagged cycles in population sizes over time (18). Indeed, in these experiments, given that the hosts are initially susceptible, we might expect large amplitude oscillations in population size, unless host resistance rapidly evolves (19). By contrast, we observed that host densities increased throughout the experiment while parasite densities remained stable (Fig. 1.A, Supplementary Text), indicating that underlying coevolutionary dynamics interfered with the expected ecological dynamics (20).

We determined whether coevolution took place in our experiment by performing 13,500 time-shift assays. This approach assesses the infectivity of parasites towards their past, present and future hosts, and reciprocally, the resistance of hosts to their past, present and future parasites (21). Resistance was measured using inhibition assays where individual host genotypes were challenged with parasite communities and resultant growth or inhibition was analysed to compare the mean levels of resistance among treatments. Infectivity and resistance varied widely across individual host-parasite communities over time (Fig. S1). Despite this complexity, two clear and significant patterns emerged. First, parasites from the future were more infective than parasites from the present or past (Fig. 1.B). Likewise, hosts

evolved increased resistance over time (Fig. 1.C). This pattern is typical of Arms Race dynamics, commonly seen with *in vitro* bacteria-phage coevolution (5, 22). Second, bacterial resistance increased with parasite diversity, while parasite infectivity decreased ( $F_{2,85}=9.7$ ,  $P < 0.001$ ), suggesting that parasite communities impose stronger selection on their host than single parasites alone.

To test the hypothesis that parasite diversity accelerated coevolution at a molecular level, we sequenced entire host and parasite populations longitudinally at multiple time points (Ancestor, Midpoint and Endpoint) from the High (N=12), Medium (N=10), Low (N=15) and Control (N=10) treatments. We could thus detect any mutations that arose during coevolution and estimate their frequency changes within populations. In the hosts, we observed 474 non-synonymous and 75 synonymous polymorphisms across 173 genes and 133 intergenic mutations. Parallel evolution with mutations in the same genes or genes in the same pathways was common across all treatments: >50% of mutations occurred in <5% of these genes. Notably, we observed parallel evolution in genes that are known phage receptors (Table S1), including LPS (N=190 mutations), Type IV pili (N=69 mutations) and the TonB dependent receptor (N=55 mutations). To measure the rate of bacterial molecular evolution, we calculated the Euclidean genetic distance of each population from the ancestor (Fig. 2.A). We found that higher levels of parasite diversity drove greater host divergence from the ancestor, and consequently faster host evolution (Fig. S2; ANOVA  $F_{2,34}=10.5$ ,  $P < 0.001$ ; Post hoc Tukey test  $P < 0.05$ ).

Two mechanisms could explain why diverse parasite communities accelerate the rate of host evolution. On one hand, diverse communities are more likely, by chance alone, to contain parasites that drive rapid evolution. On the other hand, it is possible that parasite diversity *per*

*se* accelerates host evolution by increasing selection for resistance. To discriminate between these mechanisms, we calculated the contribution of parasite diversity to the speed of host evolution by adopting an approach developed to determine the contribution of biodiversity to ecosystem function, here represented by host evolutionary rate (23). Using this approach, we found that relative to phage monocultures, the combination of all five parasites contributed to faster host evolution overall ( $D_{\max} > 0$ ; Bonferroni corrected one-sample t-tests  $P < 0.05$ ). Thus, the diversity of interactions between parasites within communities, and not merely the presence of a particular parasite, imposed stronger selection.

Whole genome sequencing also revealed profound changes in parasite communities. At an ecological level, the composition of communities changed markedly over time (Fig. S3). Parasite diversity decreased in both the medium and high diversity treatments, but diversity remained higher in the high diversity than in the medium diversity treatments (Fig. S4). At a genetic level, we found evidence for rapid molecular evolution of phage, which supports the results of our phenotypic assays. In total, we detected 533 SNPs across all five parasite types that reached  $>10\%$  in frequency in their populations (Table S2). The proportions of non-synonymous SNPs were very high, exceeding 0.7 for each parasite (Table S3), and parallel evolution was common, implying that these SNPs were predominantly beneficial mutations. To investigate the role of parasite diversity in phage evolution, we focused our analysis on communities that included the parasite PEV2, as this phage was well-represented at all levels of parasite diversity, and compared with the other phages used here, the PEV2 genome is well-annotated. For example, all but two of the genes in the parasite 14-1 genome are hypothetical proteins. We detected 225 mutations in the PEV2 genome, and the rate of PEV2 evolution was independent of parasite diversity (Fig. S5). Thirty-nine percent ( $N=88$ ) of the PEV2 mutations occurred in a single tail fibre gene, *gp52*. The tail fibers are the means by

which the parasite recognizes and binds to its receptor and are known to undergo coevolution (24). We detected mutations in *gp52* and at least one host LPS mutation (usually in *wzz* or *migA*) in every community containing PEV2 across all levels of parasite diversity (Fig. S6 and Fig. S7). Collectively, these results provide genetic confirmation for reciprocal coevolution between host and parasite across all levels of parasite diversity, and they provide further evidence that parasite attachment to LPS is a key mechanism underpinning coevolution between PEV2 and *P. aeruginosa*.

Coevolutionary dynamics are usually described as being one of two types. Arms Races occur when selection results in directional increases in host resistance and parasite infectivity (25, 26) and with Red Queen dynamics, negative frequency-dependent selection causes fluctuations in allele frequencies (27, 28). When interacting with this host in a pairwise fashion it has been previously shown that each parasite follows a different coevolutionary trajectory (29) (Fig. S8). Using a population genomic approach, we therefore sought to examine whether parasite diversity altered the mode of coevolution.

We examined the type of coevolution occurring in each community by comparing the change in frequencies of each host allele between the mid- and end-points of the experiment (29, 30). These timeframes were previously shown to be suitable for observing coevolutionary dynamics in *P. aeruginosa*-phage interactions (29). We focused our analysis on the host because changes in the frequency of phage alleles in diverse communities might additionally be driven by interspecific competition among parasites (14). On average, host alleles with higher frequencies tended to decline over time in the low and medium parasite diversity treatments, consistent with negative frequency-dependent selection on host resistance genes (Fig. 3.). This mode of selection becomes less predominant at higher levels of parasite

diversity (ANCOVA  $F_{2,335} = 12.64$ ,  $P < 0.0001$ ) suggesting that the occurrence of Red Queen dynamics was reduced in these communities.

In contrast to Red Queen dynamics, Arms Races should result in recurrent selective sweeps of resistance mutations (5). The effects of directional selection in host-parasite interactions have been studied in a variety of systems and can be important for human disease coevolution (31–34). To test for selective sweeps in host populations, we calculated  $F_{ST}$ , which measures the genetic divergence per mutation between each coevolved host population and a sequenced ancestor (35), and we set a conservative threshold  $F_{ST}$  above which any mutation was deemed to be under strong directional selection (Fig. 4.A). Strong directional selection was more common as parasite diversity increased ( $\chi^2 = 20$ ,  $df = 3$ ,  $P < 0.001$ ) such that the number of fixed alleles in the high diversity treatment was over two-fold that observed under medium diversity (Fig. 4.B). Of the 29 alleles approaching fixation, 23 were in genes relating to LPS biosynthesis. LPS is very abundant on the bacterial cell surface, and phage may initially bind to LPS to anchor themselves to the cell before forming an irreversible attachment to a final receptor (36). Mutations that alter LPS biosynthesis may provide a general phage resistance mechanism. We have previously shown that mutations in LPS biosynthesis gene *wzy* provide resistance to four of the phages used in this study (14). Red Queen and Arms Race dynamics fall at two ends of a continuum (21), with tight interaction specificity required for the former, and for the latter, general host resistance mechanisms should evolve to allow future hosts to resist all previous parasite genotypes. Our data points to that the availability of generalist LPS biosynthesis resistance mutations as key to the transition from Red Queen to Arms Race dynamics as parasite diversity increases. That both dynamics can arise from host-parasite community coevolutionary interactions are consistent with studies of bacteria-phage systems conducted in natural communities (16, 17).



Parasites have been shown to play a key role in evolutionary diversification within (37–39) and among host populations (40). Specifically, parasite-mediated selection against common host genotypes is predicted to stably maintain genetic diversity (31, 41). Host population genetic diversity should be greatest during pairwise coevolution where we observed Red Queen dynamics are relatively stronger. Surprisingly, we found that levels of genetic diversity within host populations were not impacted by parasite diversity (Fig. S9) despite the different modes of selection acting across treatments. Parasite diversity, conversely, had a profound impact on allopatric diversification among host populations (ANOSIM  $R = 0.11$   $P < 0.01$ ). The greatest divergence was found in the high parasite diversity treatment (Fig. 2.B; ANOVA  $F_{2,213} = 122.15$ ,  $P < 0.001$ ; Post-hoc Tukey test  $P < 0.05$ ). The simplest explanation for this result is that rapid evolution within host populations leads to accelerated divergence among populations.

Our study reveals that parasite communities can form hotbeds of rapid antagonistic coevolution. Relative to single parasites, diverse parasite communities imposed stronger selection on host populations, causing faster selective sweeps of generalist resistance mutations and higher levels of host resistance. The multi-species coevolutionary process ultimately accelerated the rate of molecular evolution within host populations and increased the genomic divergence among populations. Host resistance to parasite infection can be specialized (26). However, diverse, broad-spectrum defence strategies which confer protection against different enemies are widespread in animals (42–44) and plants (45, 46), as well as bacteria (47–49). We should thus consider looking beyond the pairwise towards parasite communities as drivers of coevolution and rapid host evolution in nature. This focus

could be particularly informative in biodiversity hotspots with elevated evolutionary and speciation rates (27): a multitude of parasites might be the fuel.

## References and Notes:

1. S. Paterson *et al.*, Antagonistic coevolution accelerates molecular evolution. *Nature*. **464**, 275–8 (2010).
2. J. B. S. Haldane, Disease and evolution. *La Ric. Sci.* **19**, 68–76 (1949).
3. G. Bell, *The masterpiece of nature : the evolution and genetics of sexuality* (Croom Helm, London, 1982).
4. W. D. Hamilton, Sex versus Non-Sex versus Parasite. *Oikos*. **35**, 282 (1980).
5. M. A. Brockhurst *et al.*, Running with the Red Queen: the role of biotic conflicts in evolution. *Proc. R. Soc. B.* **281**, 1–9 (2014).
6. D. J. Marcogliese, Parasites of the superorganism: Are they indicators of ecosystem health? *Int. J. Parasitol.* **35**, 705–716 (2005).
7. P. J. Hudson, A. P. Dobson, K. D. Lafferty, Is a healthy ecosystem one that is rich in parasites? *Trends Ecol. Evol.* **21**, 381–385 (2006).
8. S. Telfer *et al.*, Species interactions in a parasite community drive infection risk in a wildlife population. *Science*. **330**, 243–246 (2010).
9. E. C. Griffiths, A. B. Pedersen, A. Fenton, O. L. Petchey, The nature and consequences of coinfection in humans. *J. Infect.* **63**, 200–206 (2011).
10. J. Lello, Coinfection: doing the math. *Sci. Transl. Med.*, **5**, 191fs24 (2013).
11. S. Alizon, J. C. de Roode, Y. Michalakis, Multiple infections and the evolution of virulence. *Ecol. Lett.* **16**, 556–567 (2013).
12. F. Bashey, H. Hawlena, C. M. Lively, Alternative paths to success in a parasite community: Within-host competition can favor higher virulence or direct interference. *Evolution*. **67**, 900–907 (2013).

13. A. Betts, C. Rafaluk, K. C. King, Host and Parasite Evolution in a Tangled Bank. *Trends Parasitol.* **32**, 863–873 (2016).
14. A. Betts, D. R. Gifford, R. C. MacLean, K. C. King, Parasite diversity drives rapid host dynamics and evolution of resistance in a bacteria-phage system. *Evolution.* **70**, 969–978 (2016).
15. J. E. Samson, A. H. Magadán, M. Sabri, S. Moineau, Revenge of the phages: defeating bacterial defences. *Nat. Rev. Microbiol.* **11**, 675–87 (2013).
16. B. Koskella, N. Parr, The evolution of bacterial resistance against bacteriophages in the horse chestnut phyllosphere is general across both space and time. *Philos. Trans. R. Soc. Lond. B. Biol. Sci.* **370**, 20140297 (2015).
17. P. Gómez, A. Buckling, Bacteria-phage antagonistic coevolution in soil. *Science.* **332**, 106–109 (2011).
18. P. J. Hudson, A. P. Dobson, D. Newborn, Prevention of Population Cycles by Parasite Removal. *Science.* **282**, 2256–2258 (1998).
19. A. Mougi, Y. Iwasa, Evolution towards oscillation or stability in a predator-prey system. *Proc. R. Soc. B.* **277**, 3163–71 (2010).
20. M. H. Cortez, J. S. Weitz, Coevolution can reverse predator-prey cycles. *Proc. Natl. Acad. Sci.* **111**, 7486–91 (2014).
21. S. Gandon, A. Buckling, E. Decaestecker, T. Day, Host-parasite coevolution and patterns of adaptation across time and space. *J. Evol. Biol.* **21**, 1861–6 (2008).
22. A. Buckling, Y. Wei, R. C. Massey, M. A. Brockhurst, M. E. Hochberg, Antagonistic coevolution with parasites increases the cost of host deleterious mutations. *Proc. R. Soc. B.* **273**, 45–49 (2006).

23. M. Loreau, A. Hector, Biodiversity and Ecosystem Functioning : Current Knowledge and Future Challenges. *Science*. **294**, 804–809 (2001).
24. J. S. Weitz, H. Hartman, S. A. Levin, Coevolutionary arms races between bacteria and bacteriophage. *Proc. Natl. Acad. Sci.* **102**, 9535–9540 (2005).
25. A. Buckling, P. B. Rainey, Antagonistic coevolution between a bacterium and a bacteriophage. *Proc. R. Soc. B.* **269**, 931–936 (2002).
26. A. Agrawal, C. Lively, Infection genetics: gene-for-gene versus matching-alleles models and all points in between. *Evol. Ecol. Res.* **4**, 79–90 (2002).
27. M. D. Pirie *et al.*, The biodiversity hotspot as evolutionary hot-bed: spectacular radiation of *Erica* in the Cape Floristic Region. *BMC Evol. Biol.* **16**, 190 (2016).
28. E. Decaestecker *et al.*, Host-parasite “Red Queen” dynamics archived in pond sediment. *Nature*. **450**, 870–873 (2007).
29. A. Betts, O. Kaltz, M. E. E. Hochberg, Contrasted coevolutionary dynamics between a bacterial pathogen and its bacteriophages. *Proc. Natl. Acad. Sci.* **111**, 11109–11114 (2014).
30. B. Koskella, C. M. Lively, Evidence for negative frequency-dependent selection during experimental coevolution of a freshwater snail and a sterilizing trematode. *Evolution*. **63**, 2213–21 (2009).
31. R. D. Schulte, C. Makus, B. Hasert, N. K. Michiels, H. Schulenburg, Multiple reciprocal adaptations and rapid genetic change upon experimental coevolution of an animal host and its microbial parasite. *Proc. Natl. Acad. Sci.* **107**, 7359–64 (2010).
32. L. Wilfert, F. M. Jiggins, Disease association mapping in *Drosophila* can be replicated in the wild. *Biol. Lett.* **6**, 666–668 (2010).

33. B. Roche *et al.*, Might Interspecific Interactions between Pathogens Drive Host Evolution? The Case of Plasmodium Species and Duffy-Negativity in Human Populations. *Trends Parasitol.* **33**, 21–29 (2017).
34. C. Eizaguirre, T. L. Lenz, M. Kalbe, M. Milinski, Divergent selection on locally adapted major histocompatibility complex immune genes experimentally proven in the field. *Ecol. Lett.* **15**, 723–731 (2012).
35. S. Wright, *Evolution and the Genetics of Populations* (University of Chicago Press, Chicago, IL, 1969), vol. 2, 1-295.
36. S. T. Abedon, *The Bacteriophages* (Oxford, ed. 2, 2006).
37. K. C. King, L. F. Delph, J. Jokela, C. M. Lively, The Geographic Mosaic of Sex and the Red Queen. *Curr. Biol.* **19**, 1438–1441 (2009).
38. M. F. Marston *et al.*, Rapid diversification of coevolving marine *Synechococcus* and a virus. *Proc. Natl. Acad. Sci.* **109**, 4544–4549 (2012).
39. L. T. Morran, O. G. Schmidt, I. A. Gelarden, R. C. Parrish, C. M. Lively, Running with the Red Queen: host-parasite coevolution selects for biparental sex. *Science.* **333**, 216–218 (2011).
40. J. Thompson, *Geographic Mosaic of Coevolution* (The University of Chicago Press, Chicago, IL, 2005).
41. V. M. D’Costa *et al.*, Antibiotic resistance is ancient. *Nature.* **477**, 457–61 (2011).
42. J. Klein, C. O’Huigin, MHC Polymorphism and Parasites. *Philos. Trans. R. Soc. B Biol. Sci.* **346**, 351–358 (1994).
43. A. B. Duncan, S. Fellous, O. Kaltz, Reverse Evolution : Selection Against Costly Resistance In Disease-Free Microcosm Populations Of *Paramecium Caudatum*.

- Evolution*. **65**, 3462–3474 (2011).
44. G. Tetreau, R. Stalinski, J. David, L. Després, Increase In Larval Gut Proteolytic Activities And Bti Resistance In The Dengue Fever Mosquito. *Arch. Insect Biochem. Physiol.* **82**, 71–83 (2013).
  45. V. Nicaise, Crop immunity against viruses: outcomes and future challenges. *Front. Plant Sci.* **5** (2014).
  46. L. G. Barrett, F. Encinas-viso, J. J. Burdon, P. H. Thrall, Specialization for resistance in wild host-pathogen interaction networks. *Front. Plant Sci.* **6**, 1–13 (2015).
  47. F. Rodriguez-Valera *et al.*, Explaining microbial population genomics through phage predation. *Nat. Rev. Microbiol.* **7**, 828–836 (2009).
  48. S. Avrani, O. Wurtzel, I. Sharon, R. Sorek, D. Lindell, Genomic island variability facilitates Prochlorococcusvirus coexistence. *Nature*. **474**, 604–608 (2011).
  49. S. Doron *et al.*, Systematic discovery of antiphage defense systems in the microbial pangenome. *Science*. **359** (2018), doi:10.1126/science.aar4120.
  50. R. R Development Core Team, R. D. C. Team, Ed., R: A Language and Environment for Statistical Computing. *R Found. Stat. Comput.* **1**, 409 (2011).
  51. G. L. Winsor *et al.*, Pseudomonas Genome Database : improved comparative analysis and population genomics capability for Pseudomonas genomes. *Nucleic Acids Res.* **39**, 596–600 (2011).
  52. R. Kofler *et al.*, PoPoolation2 : identifying differentiation between populations using sequencing of pooled DNA samples ( Pool-Seq ). *Bioinformatics*. **27**, 3435–3436 (2011).
  53. H. Li *et al.*, The Sequence Alignment/Map format and SAMtools. *Bioinformatics*. **25**,

2078–2079 (2009).

- 54. A. A. Popescu, K. T. Huber, E. Paradis, Ape 3.0: New tools for distance-based phylogenetics and evolutionary analysis in R. *Bioinformatics*. **28**, 1536–1537 (2012).
- 55. M. Loreau, Separating sampling and other effects in biodiversity experiments. *Oikos*. **82**, 600–602 (1998).
- 56. B. C. Sheldon, S. Verhulst, Ecological immunology - costly parasite defenses and trade- offs in evolutionary ecology. *Trends Ecol. Evol.* **11**, 317–321 (1996).



**Acknowledgments:**

We thank Michael Brockhurst, Dylan Dahan, Kevin Foster, Owen Lewis and Steve Paterson for their helpful comments. We also thank the High-Throughput Genomics Group at the Wellcome Trust Centre for Human Genetics funded by Wellcome Trust grant reference 090532/Z/09/Z and Medical Research Council Hub grant G0900747 91070 for generation of the high-throughput sequencing data. AB was supported by DPhil funding from the Biotechnology and Biological Sciences Research Council (BBSRC) [grant number BB/J014427/1]. R.C.M was funded by the Royal Society, European Research Council grant 281591, and Wellcome Trust Grant 106918/Z/15/Z. KCK was supported by a Leverhulme Research Project Grant RPG-2015-165.

The host and parasite sequences reported in this paper have been deposited in the National Center for Biotechnology (NCBI) database, [www.ncbi.nlm.nih.gov](http://www.ncbi.nlm.nih.gov) (accession numbers PRJNA448325 and PRJNA448370 respectively). All other data are available in the supplementary materials.

AB, RCM, and KCK conceived and designed the study. AB and MZ collected the data. AB and CG conducted the data analysis. AB, RCM, and KCK drafted the article, with critical revisions provided by all authors.

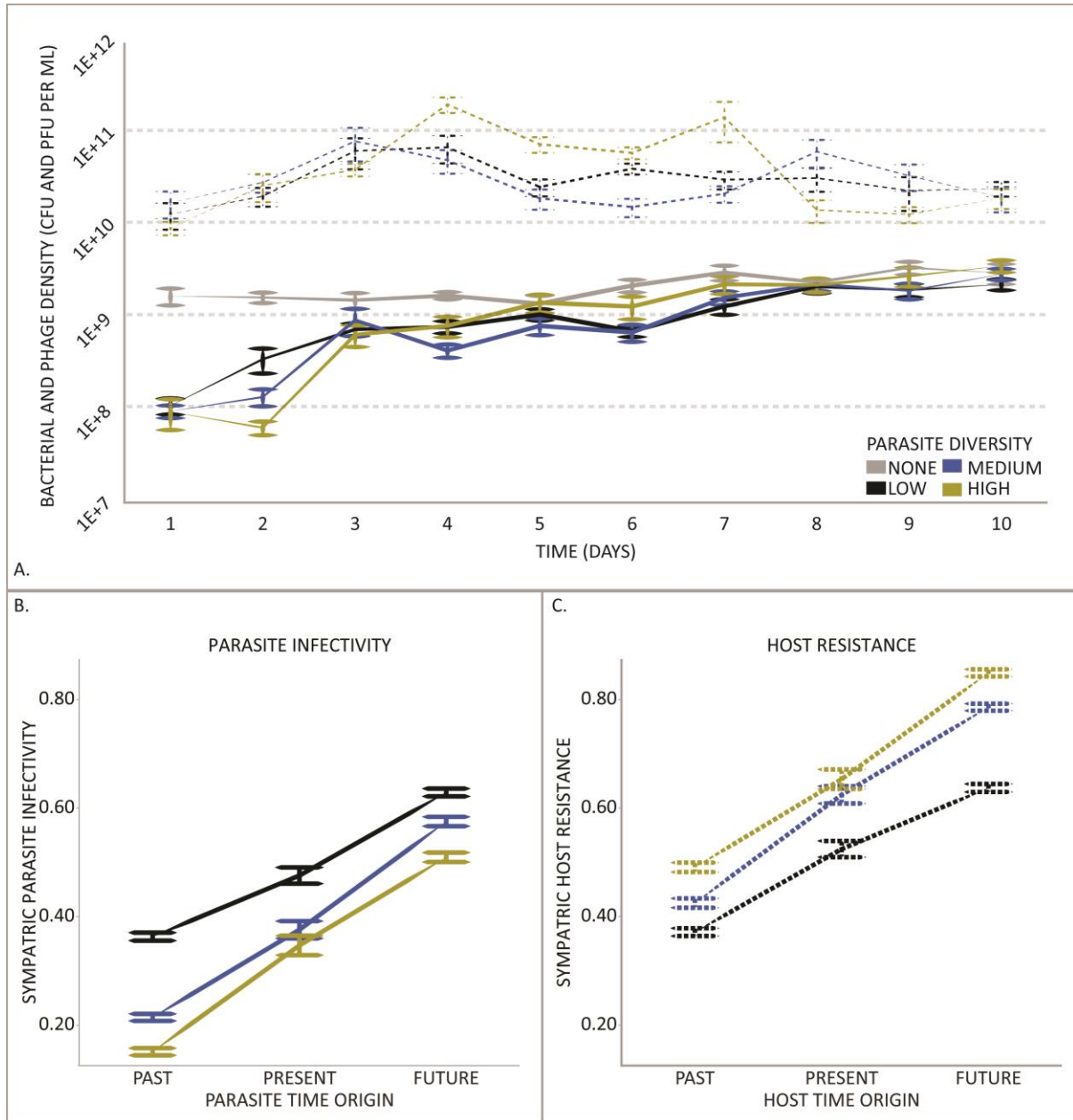


**Fig. 1.** Ecological and Coevolutionary Dynamics of Host-Parasite Interactions. **(A)** We tracked the population dynamics of hosts (solid lines) and parasites (dashed lines) for high (yellow), medium (blue) and low (black) diversity populations alongside the parasite free control (grey). All plotted points show the mean  $\pm$  standard error population density. Bacterial populations challenged with phage rapidly recovered their density. We did not observe cyclical oscillations in host and parasite densities. **(B and C)** To directly test for co-evolution, we used 13,500 time shift assays to measure changes in phage infectivity and bacterial resistance to phage. Lower levels of parasite infectivity **(B)** and higher levels of host

resistance (C) evolve with increasing parasite diversity ( $F_{2,85} = 9.7$ ,  $P < 0.001$ ). Furthermore, hosts are more susceptible to parasites from their future than their contemporary parasites and they are most resistant to parasites from their past. Likewise future parasite are more infective than past or contemporary parasites ( $F_{2,13044} = 1766.21$ ,  $P < 0.0001$ ). Error bars show 1 standard error.

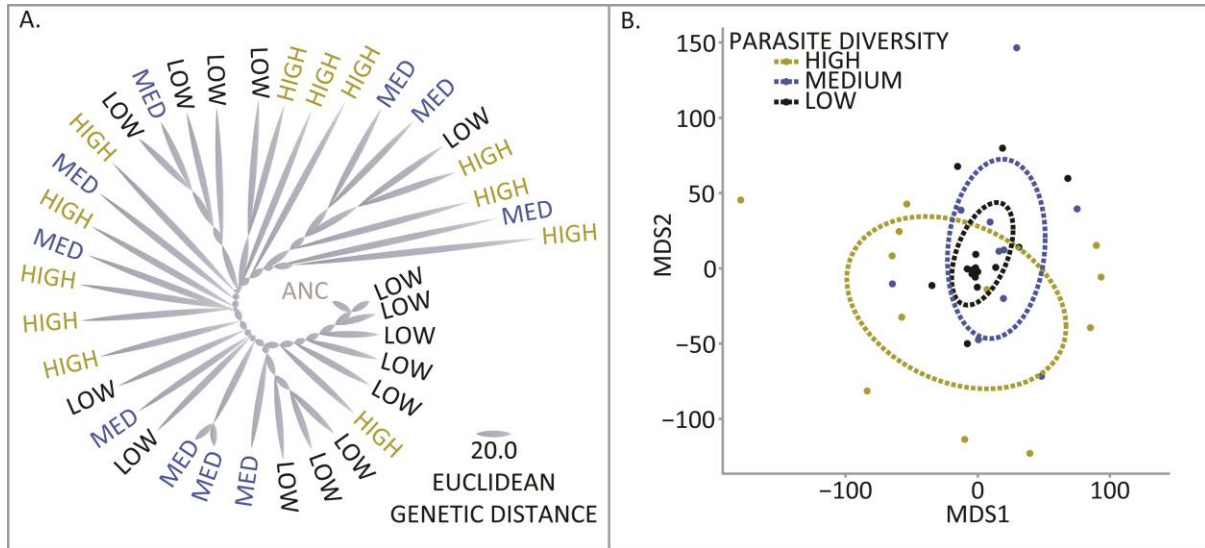


**Fig. 2.** Parasite diversity accelerates host evolution **(A)** Host allele frequencies after 10 days of coevolution from the high (yellow), medium (blue) and low (black) parasite diversity treatments were used to calculate pairwise Euclidean distances between the ancestral sequence (grey) and each coevolved population. Increasing parasite diversity accelerated the rate of host evolution. **(B)** The genetic distances between coevolved populations were ordinated by non-metric multidimensional scaling. The ellipses represent a 95% confidence bubble around the means for the different treatments. We found evidence of divergence between populations within treatments (ANOSIM  $R = 0.11$   $P < 0.01$ ), and the greatest within treatment diversification was observed in the high parasite diversity treatment.

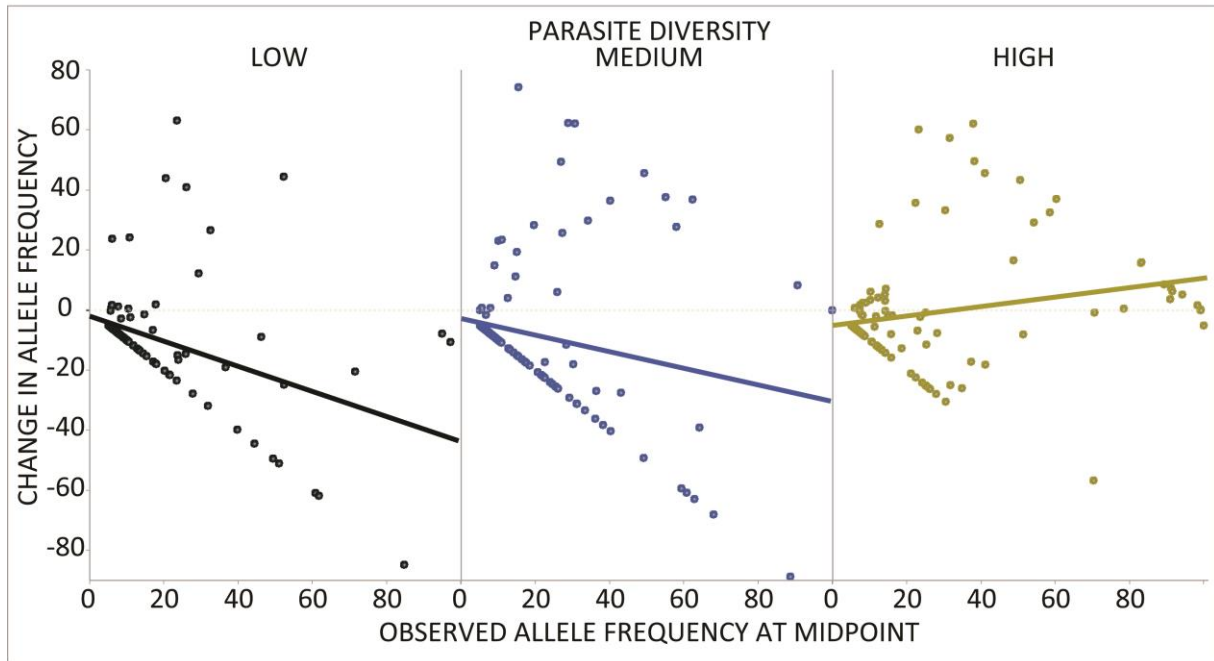


**Fig. 3.** Red Queen coevolution more common in pairwise host-parasite interactions. We tested for Red Queen dynamics by regressing the change in host allele frequency from day 5 to day 10 (y-axis) with observed frequency on day 5 (x-axis). We found evidence for negative frequency dependent selection on host alleles under low (black) and medium (blue) parasite diversity, but not at high parasite diversity (yellow). The string of points forming a straight downward slope from zero in all three panels are alleles observed on day 5 that had subsequently decreased in frequency to below our ability to detect them at day 10.

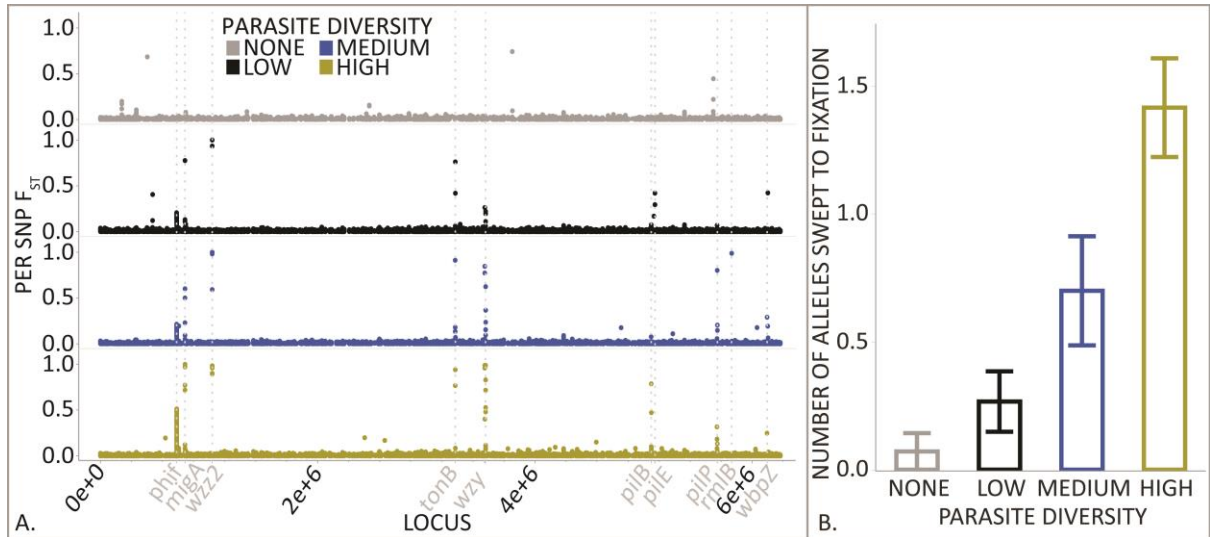


**Fig. 4.** Parasite diversity leads to more Arms Race coevolutionary dynamics. (A) To test for Arms Race Dynamics, we calculated  $F_{ST}$  for all host SNPs across the *P. aeruginosa* genome across the high (yellow), medium (blue) and low (black) parasite diversity treatments and the parasite free control (grey). Each plotted point in the panel represents a single SNP and host genes that are known parasite targets are shown in italics, including genes involved in LPS biosynthesis, Type IV pili biosynthesis, and the Ton-B dependent receptor. (B) We used a conservative  $F_{ST}$  cutoff to identify selective sweeps of SNPs per host population (+/- standard error), and we found that increasing parasite diversity increased the rate of fixation of SNPs ( $\chi^2 = 20$ ,  $df = 3$ ,  $P < 0.001$ ).



## Supplementary Materials for

### High Parasite Diversity Accelerates Host Adaptation And Diversification

**Authors:** A. Betts<sup>1\*</sup>, C. Gray<sup>2</sup>, M. Zelek<sup>1</sup>, R.C. MacLean<sup>1+</sup>, K.C. King<sup>1+</sup>.

**Affiliations:**

<sup>1</sup>Department of Zoology, University of Oxford, South Parks Road, Oxford OX1 3PS, UK

<sup>2</sup>Department of Life Sciences, Imperial College London, Silwood Park Campus, Ascot, SL5 7PY, UK

\*Correspondence to: [Alex.Betts@evobio.eu](mailto:Alex.Betts@evobio.eu), [Kayla.King@zoo.ox.ac.uk](mailto:Kayla.King@zoo.ox.ac.uk)

<sup>+</sup> contributed equally

**This PDF file includes:**

Materials and Methods  
SupplementaryText  
Figs. S1 to S9  
Tables S1 to S4  
References 50-56

## Materials and Methods

### Isolates and bacteriophage characteristics

Independent isogenic lineages of *Pseudomonas aeruginosa* PAO1 (referred to as the ancestors) were prepared from single colonies with a common ancestor and preserved as stocks of approximately 107 CFU/ml at -80°C with 25% glycerol. Five bacteriophage types were used, three from the Podoviridae (PEV2, LUZ19 and LUZ7) and two from the Myoviridae (1411 and LMA2). All five ancestral phage strains were stored as stocks of approximately 108 PFU/ml at 4°C.

### Experimental coevolution

Combinations of the five phages (one-phage monocultures, every possible two-phage combination, and a five-phage community alongside a phage-free control) were prepared such that the phages were at an inoculation titre of  $5 \times 10^5$  PFU mL<sup>-1</sup> and within mixed phage communities, each phage type was present in equal densities. These communities were then mixed with *P. aeruginosa* cultured overnight in KB. Each culture was prepared from a separate ancestral colony and used to inoculate each replicate to a starting concentration of  $5 \times 10^7$  colony forming units per mL (CFU mL<sup>-1</sup>). These experiments were conducted in 5 ml round bottom polystyrene test tubes with vented caps (Corning, Flintshire, UK) containing 2.5 ml of King's B (KB) culture medium (microcosms). These microcosms were incubated at 37°C and 2250-RPM orbital agitation in a MaxQ 8000 shaker-incubator (Thermo Scientific, Waltham, MA, USA). This experiment was designed to include a blocking structure, with three sequential batches each of 40 lineages. Within each batch, replicates were evenly separated across the three levels of phage diversity (One, Two and Five-phage) and the phage three control such that each treatment had 10 replicates per batch. For each replicate, a 50µl sample containing both bacteria and phage were serially transferred to a new microcosm every 24 hours. Each batch underwent ten such transfers. At each transfer, a 500µl sample was taken and stored in 50% glycerol at -80°C for subsequent analysis.

### Measuring host and parasite community density

Every 24 hours samples were taken from each replicate to allow hosts and parasites to be enumerated. Samples were serially diluted and plated via a previously used soft KB agar overlay method to allow the counting of individual phage plaque forming units (PFU) on a lawn of susceptible *P. aeruginosa* PAO1 from which phage population density (PFU/ml) can be estimated. These diluted samples were simultaneously plated on KB agar to display single bacterial colony forming units (CFU/ml) from which bacterial population density was estimated.

Host and parasite community densities (Fig. 1.A) were analysed using separate linear mixed effects models. We fitted the maximal model with parasite diversity and transfer as interacting fixed effects, and batch, parasite community and replicate as nested random effects. The model was simplified using stepwise model simplification based on AIC. A 2-parameter autocorrelation-moving average correlation structure was built in to the host density model. Post-hoc contrasts were performed using Tukey HSD tests.

### Measuring parasite infectivity and host resistance

Using a sterile 1 µL inoculation loop, coevolved populations were streaked out onto KB agar. These plates were then placed in a static incubator overnight at 37°C to allow the growth of individual colonies. Some such colonies were picked with another loop and similarly streaked out and incubated to present single colonies which enables the isolation of phage free, isogenic bacterial populations from the evolved communities. Isolates from each



replicate were used to inoculate individual microcosms incubated for 24 hours. Subsequently a 100  $\mu$ L sample from each microcosm was mixed with 2.9 mL of molten KB agar (0.75% agar) and spread evenly over the surface of a KB agar (1.5% agar) plate. These soft agar lawns were then inoculated with 4  $\mu$ L droplets of purified phage, which were allowed to dry, and then incubated for 24 hours. This period allowed the formation of zones of inhibition, which indicated susceptibility or resistance. Droplets which produced with no visible inhibition were scored as resistant (=1), those with some visible inhibition were scored as partially resistant (=0.5), and those with complete inhibition were scored as susceptible (=0). These data were then analysed as the proportion of clones that were resistant or susceptible to a given phage isolate.

#### Time shift assays: Detecting coevolution between bacteria and phages

A time-shift assay approach enabled the detection of adaptations and counter-adaptations that coevolved during the serial transfer experiment. Bacterial resistance was measured against phage from the same lineage (sympatric), isolated from past, present and future transfers. Likewise, the infectivity of phage was measured on sympatric bacteria from past, present and future transfers. Escalating coevolutionary arms races between hosts and parasites are defined by successive increases in resistance and infectivity. Deviations in linearity, especially those that give rise to local minima or maxima of infectivity and resistance, indicate fluctuating selection dynamics as with the frequency-dependent selection dynamics that underlie Red Queen coevolution. A total of 13,500 combinations of coevolved bacterial genotypes and phage communities were assayed during the time-shift comparing the resistance of bacteria from 24, 120 and 240 hours to the phage communities with which they had coevolved from 10 time points, every 24 hours between 24 and 240 hours. These data were categorised first by the diversity of phage with which they were coevolved and second by whether the contrast combined a bacterial genotype with its contemporary phage community, phage from its past or phage from its future. These data were then analysed in a linear mixed effects model in R (50) with bacterial genotype nested within replicate, within phage diversity, within batch as random effects and phage diversity crossed with phage time origin as fixed effects.

#### Genome resequencing analysis

Whole community DNA extractions were performed on 91 samples for sequencing. Three ancestral *P. aeruginosa* clones and 14 whole populations from the phage-free control were sequenced to enable the identification of mutations resulting from laboratory adaptation and any differences in the ancestor from the published reference sequence (NC\_002516.2). In total, 15 one-phage, 10 two-phage and 12 five-phage replicates were sampled longitudinally at two time points (5 days and 10 days) so that allele frequency changes within populations could be easily observed. A subsample of these populations which included the phage PEV2 were analysed to confirm molecular evolution in the bacteriophage. PEV2 was chosen as its reference genome was most recently sequenced and is comparatively well annotated for a bacteriophage genome, all of the phages used here have published reference genomes (KU948710.1, NC\_013691, NC\_010326, NC\_011703 & NC\_011166) but the vast majority of genes are of unknown function, for example; all but two of the genes in the parasite 14-1 are hypothetical proteins. In the case of PEV2, more than one gene relating to tail fibre production has been identified and tail fibres are known to be an important structure under selection during antagonistic coevolution between phage and bacteria. The parasites used here all have sequenced reference genomes against which any sequenced reads could be mapped (KU948710.1, NC\_013691, NC\_010326, NC\_011703 & NC\_011166). We used coverage data from the Phage mappings to estimate the relative composition of each

community at different time points by using the number of mapped reads as a proxy for relative abundance. We selected 2 PEV2 low diversity replicates, 4 medium diversity replicates (one each in which PEV2 coexisted with the other four phage types) and six high diversity replicates. Each of these replicates was analysed at both the mid and endpoint of the experiments.

Whole community DNA extractions were performed on 1ml of culture using a DNeasy Blood and Tissue kit (Qiagen, Inc., Chatworth, California, USA), quantified using the QuantiFluor dsDNA system (Promega, Madison, WI, USA) and the salt ratio verified by Nano Drop (Thermo Scientific, Waltham, MA, USA). Whole genome sequencing services were provided by the Wellcome Trust Centre for Human Genetics (Oxford, UK) using the Illumina HiSeq platform with 150 bp paired-end reads. All mapping and variant calling was performed using CLC genomics Workbench (CLC Bio). First, 5' or 3' ends were trimmed if the Phred quality score was less than 20. Reads were discarded if they were shorter than 50 bp after trimming or if more than 2 bases were ambiguous. Filtered reads were then mapped to the *P. aeruginosa* PA01 reference genome or the Pseudomonas phage PEV2 reference genome. Mapped reads were then processed to increase the quality of the variant calling; duplicated reads were discarded and reads around indels were locally realigned. A Neighbourhood Quality Standard model was then applied to detect single nucleotide polymorphisms and a separate model was used concurrently to detect deletion/insertion polymorphisms. Variants were then filtered to remove any also present in the three sequenced ancestral clones or one ancestral phage population, thus ensuring that all reported SNPs are certain to have arisen during the experiment, not before. Finally, variants in the host samples were annotated using the Pseudomonas database (51) whereas the parasite variants were annotated using the reference sequence as no larger database exists for these parasites.

#### Detecting genetic signature of coevolution using Host and Parasite SNPS

Previously published data has shown that host LPS genes and parasite tail fibre genes can be the focus of antagonistic coevolution (24). Using the SNP data collected for both the hosts and parasites we computed a gene interaction matrix for each of the subsampled replicates containing PEV2. For every possible host gene – parasite gene combination, we calculated the number of communities in which mutations in those genes co-occurred. To visualize the relationship the frequency at which a particular gene pair co-occurred was then used to weight the interactions in a host-parasite gene interaction network produced using bipartite in R showing every possible gene combination across all replicates. In the majority of cases (69%), mutations in particular host and parasite genes only co-occurred in a single replicate. By contrast, the two most common gene co-occurrences were between a parasite tail fibre gene (gp52) and either of two host LPS biosynthesis genes (wzy or mig8). These data strongly support antagonistic coevolution driven by mutations in parasite tail fiber genes and host LPS genes.

#### Detecting genomic signatures of strong directional selection

We used PoPoolation 2 (52) to calculate the per locus  $F_{ST}$  between each 10 day coevolved population and one of the three isogenic sequenced ancestors. The mapped genomes were sorted and synchronised using SAMtools (53). The  $F_{ST}$  was then calculated for every SNP genomewide using the  $F_{ST}$ -sliding tool of Population 2. The majority of the 6.3 million loci were not under strong selection in this experiment and produced very low  $F_{ST}$  values. All values  $<0.05$  were excluded and with the remaining data (mean 0.174 s.d. = 0.164) we calculated 3 standard deviations above the mean to give a conservative threshold  $F_{ST}$  of 0.67, all values higher than this were taken to be indicators of strong directional

selection driving alleles towards fixation. The number of mutations with signatures of strong directional selection was compared between treatments with a chi-squared test.

#### Determining effects of parasite diversity on evolutionary rates

The Euclidean genetic differences (the square root of pairwise differences) between each coevolved population ancestor was calculated using the frequency of detected variants. Indels varied in size but were each counted as just a single mutation. Host mutations with a frequency of <5% and parasite mutations with a frequency of <10% were not included to optimize the quality of our data sets. A phylogeny was produced on the resultant distance matrix using the library APE (54) in R (50). The significance of the differences in genetic distances between treatments was compared by ANOVA and post hoc contrasts were performed using Tukey HSD tests.

The Euclidean genetic distances between each coevolved host population were investigated by nMDS ordination and ANOSIM which partitions diversity within and between treatments and computes a value or  $R \approx 0$  when there is no difference. Secondly, the genetic distances between each coevolved host population within each diversity treatment were analysed by ANOVA followed by post hoc Tukey HSD tests. Within population diversity was estimated with Shannon's diversity index calculated from the SNP data.

We also performed the test for transgressive overyielding ( $D_{\max}$  (55)) e.g. is host evolutionary rate greater with a community of parasites A, B & C than with monocultures of either A, B or C. This confirmed if our diversity effect was due to diverse communities being more likely to contain phages which drive rapid evolution rather than a positive interaction between phages in communities accelerating coevolution. We calculated  $D_{\max}$  using the genetic distances from the high parasite diversity treatment and the genetic distances of each of the parasites in monoculture. One-sample t-tests were performed with a Bonferroni correction to test whether each phage had a  $D_{\max}$  significantly greater than zero.

### **Supplementary Text**

#### Analysis of ecological data

Parasite diversity significantly affected host population density ( $F_{3,45} = 6.59$ ,  $P < 0.001$ ). The highest host densities were achieved with high parasite diversity, but host densities increased over time regardless of parasite diversity ( $F_{1,1079} = 160.74$ ,  $P < 0.001$ ). We observed no time-dependent relationship with the parasite community densities. Indeed, the only significant factor explaining parasite densities was parasite diversity ( $F_{2,43} = 6.1$ ,  $P < 0.01$ ) with the high parasite diversity treatment reaching the highest parasite density (Post-hoc Tukey test  $P < 0.05$ ).

Accelerated resistance evolution could have important ecological consequences as parasites require susceptible hosts to complete their lifecycles (56). In the absence of any evolutionary change, we would expect parasite populations to grow with host populations. Our observation that parasite densities were stable over time despite simultaneously increasing host densities suggests feedbacks between evolutionary and ecological dynamics (19) and confirms the evolution of host resistance. That parasite densities do not subsequently decrease in the face of increasing resistance (and dilution into fresh media every 24 hours) agrees with our time shift results and could be explained by a quick coevolutionary response from the parasites allowing them to infect the new host genotypes (20).

### Analysis of time-shift data

We observed that parasite diversity significantly increased the magnitude of resistance and infectivity evolution over time ( $F_{2,85} = 9.7$ ,  $P < 0.001$ ) with the low parasite diversity treatment selecting for the least resistance and most infectivity; significantly different to the intermediate (Post-hoc Tukey test  $P < 0.05$ ) and high parasite diversity treatments (Post-hoc Tukey test  $P < 0.001$ ). The data also show significant change in the ability of parasites to infect hosts over time ( $F_{2,13044} = 1766.21$ ,  $P < 0.0001$ ). Within each level of parasite diversity, resistance was always lowest to parasites from the future and highest to parasites from the past (Post-hoc Tukey test  $P < 0.0001$ ). This pattern is typical of arms race dynamics, commonly seen in in vitro bacteria-phage interactions (5, 22). The significant interaction between parasite diversity and parasite time origin ( $F_{4,13044} = 16.99$ ,  $P < 0.0001$ ) is largely explained by the differing abilities of parasite communities to overcome evolved host resistance. Interestingly, the resistance of host populations to their contemporary parasite communities were very similar (Post-hoc Tukey test  $P > 0.2$ ) yet the resistance of the intermediate parasite diversity coevolved hosts to past and future parasites was significantly lower (Post-hoc Tukey test  $P < 0.05$ ) than the high parasite diversity coevolved hosts. These results suggest a greater ability of the host populations facing high parasite diversity to evolve resistance.

### Phage diversity PCR

The presence or absence of the five different phage types at the end of the experiment in the high parasite diversity treatment was confirmed via PCR.

Primers specific to each phage (Table S4.) were designed and tested for potential cross amplification against the *P. aeruginosa* chromosome and the other phage types used here in Geneious 6.06 (Biomatters Ltd. Auckland, NZ). All primer pairs were designed with an amplicon size of 150bp within genes thought to encode the tail fibre proteins of each phage. PCR was performed using GoTaq green Mastermix (Promega, Madison, WI, USA) on whole community DNA extracted 1ml of culture using a DNeasy Blood and Tissue kit (Qiagen, Inc., Chatworth, California, USA).

The number of phage types detected in the samples from the end of the experiment (Fig. S4.) were analysed by ANOVA. In several samples, different phage have fallen below the detection threshold, but not to the extent that our diversity treatments were compromised (ANOVA  $F_{2,34} = 38.73$ ,  $P < 0.001$ ) the high diversity treatment remains more diverse than the medium (Post-hoc Tukey test  $P < 0.0001$ ), which is in turn more diverse than the low (Post-hoc Tukey test  $P < 0.05$ ).

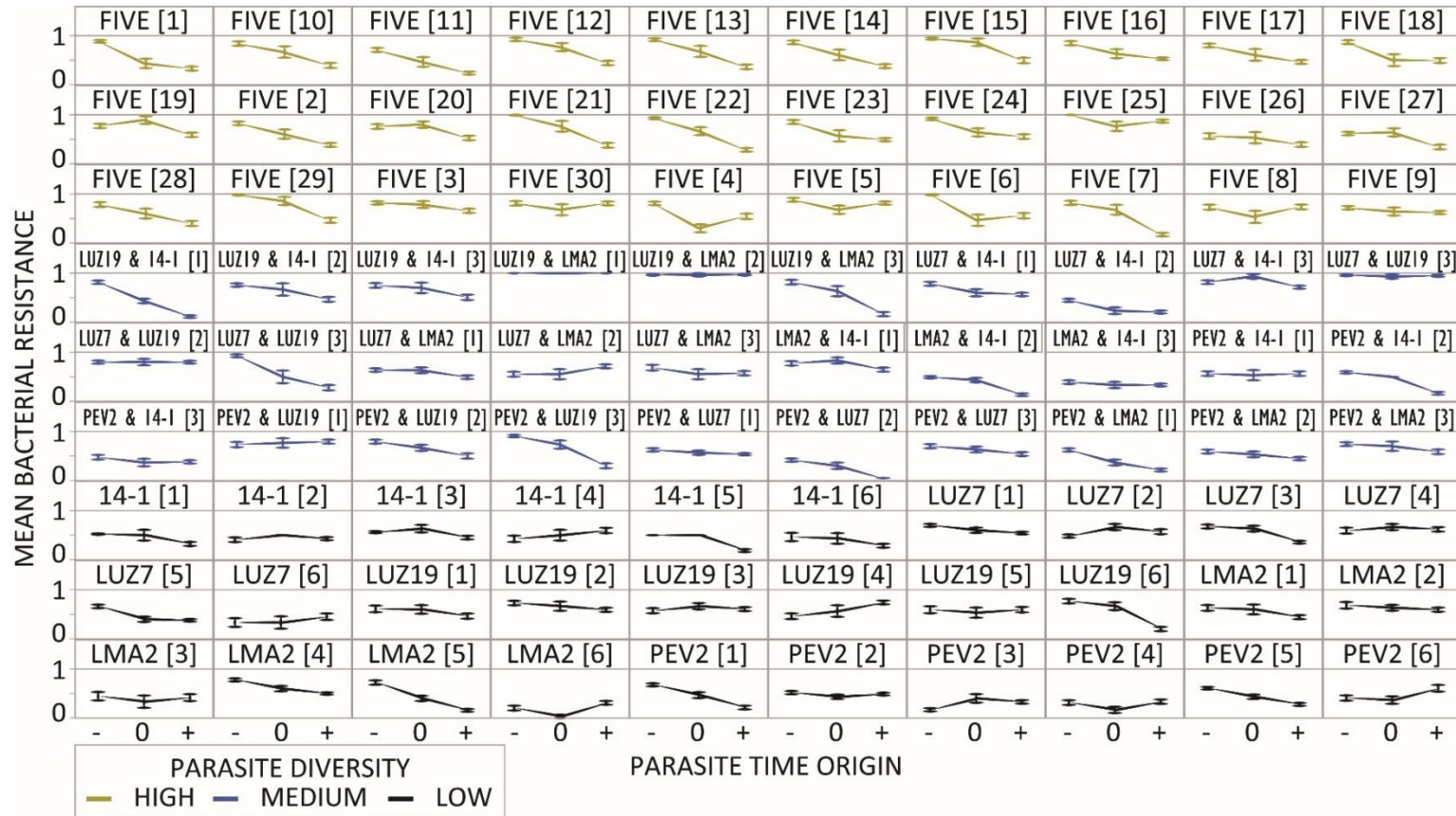


Fig. S1 Coevolutionary trajectories vary between replicates. By comparing the resistance of hosts from multiple time points to parasites from their coevolutionary past, present and future from all levels of parasite diversity (low (black), medium (blue) and high (yellow)), the pattern of phenotypic change in hosts and parasites through time can be summarised. The header for each panel lists the species of parasite present with the replicate number in square brackets. Here, individual communities displayed an incredible diversity of changes in infectivity and resistance over time. Despite this extraordinary complexity, by combining these data with our molecular data we were able to discern the effects of diversity on coevolutionary dynamics (-= parasites from host's past, 0= parasites from host's present, += parasites from host's future. Error bars indicate 1 standard error.

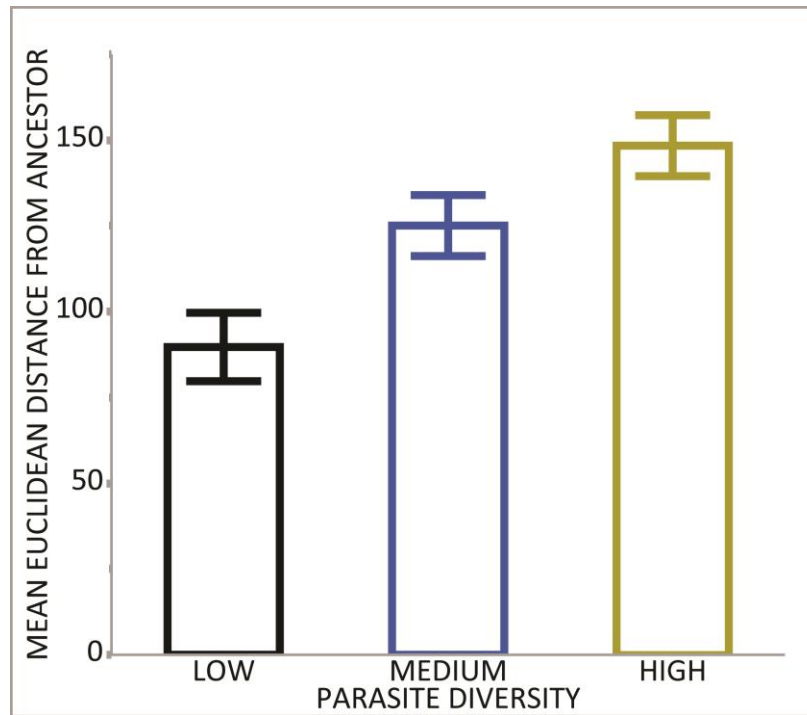


Fig. S2 Parasite diversity drives host evolution. We compared the mean Euclidean distance between the host populations that had coevolved with parasite communities of different diversities (low (black), medium (blue) and high (yellow)). Parasite diversity significantly increased evolved host distance from the ancestor (ANOVA  $F_{2,34} = 10.5$ ,  $P < 0.001$ ). The low diversity populations had the lowest mean distance from the ancestor (Post hoc Tukey test  $P < 0.05$ ). Error bars show 1 standard error.

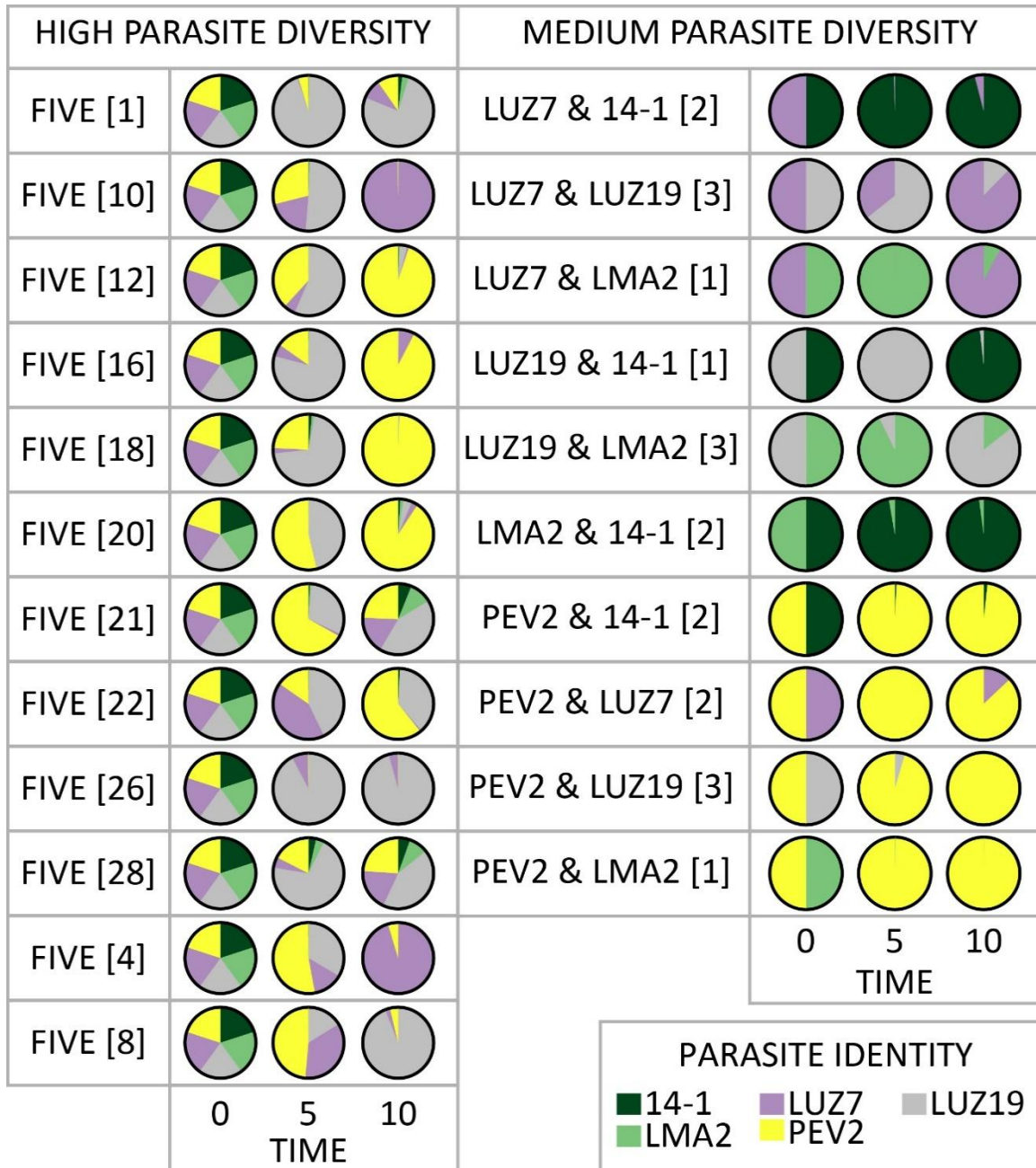


Fig. S3 A time series of parasite community composition. Each panel in this figure contains three pie charts providing snapshots of the relative composition of a parasite community from the start, mid and end-points of the experiment. The starting composition was controlled by our experimental conditions, the composition on days 5 and 10 were estimated using the number of sequencing reads that would map to the relevant genome as a proxy for relative parasite abundance. The figure shows data from the medium and high diversity treatments.



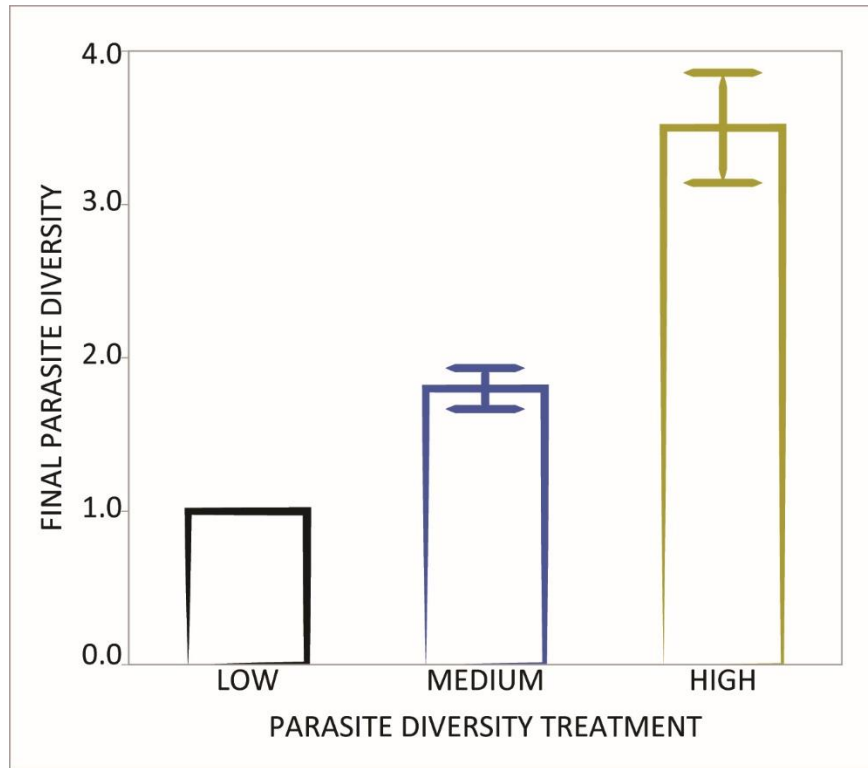


Fig. S4 Changes in parasite community diversity. To test for changes across all levels of parasite diversity (low (black), medium (blue) and high (yellow)) during coevolution we tested for the presence/absence of phage at day 10 of the evolution experiment using PCR on community genomic DNA. Bars show the mean ( $\pm$  standard error) number of phage species detected as a function of initial parasite diversity. Phage extinctions occurred in some communities, but not to the extent that our diversity treatments were compromised (ANOVA  $F_{2,34} = 38.73$ ,  $P < 0.001$ ) the high diversity treatment remains more diverse than the medium (Post-hoc Tukey test  $P < 0.0001$ ), which is in turn more diverse than the low (Post-hoc Tukey test  $P < 0.05$ ). Methods: Primers specific to each phage (Table S4.) were designed and tested for potential cross amplification against the *P. aeruginosa* chromosome and the other phage types used here in Geneious 6.06 (Biomatters Ltd. Auckland, NZ). All primer pairs were designed with an amplicon size of 150bp within genes thought to encode the tail fibre proteins of each phage. PCR was performed using GoTaq green Mastermix (Promega, Madison, WI, USA) on whole community DNA extracted 1ml of culture using a DNeasy Blood and Tissue kit (Qiagen, Inc., Chatworth, California, USA).



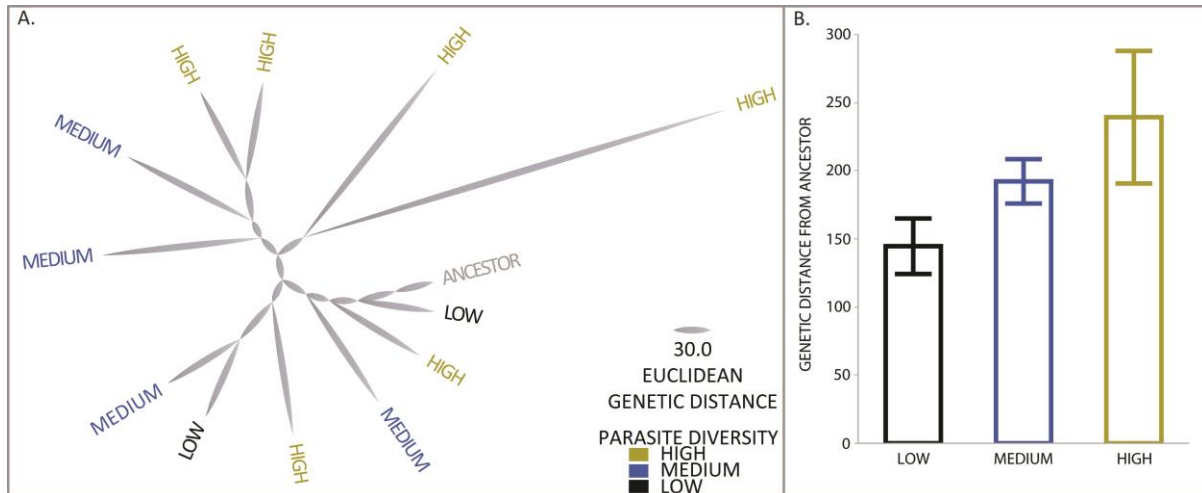


Fig. S5 Parasite diversity does not accelerate parasite evolution. (A) A tree based on Euclidean genetic distance data from our sequenced PEV2 populations from all levels of parasite diversity (low (black), medium (blue) and high (yellow)). This figure was prepared using the same methods as Fig 2(A) in the main manuscript. (B) This figure shows the mean genetic distance from the ancestor, the rate of evolution, in PEV2 across the three treatment levels. It is worth noting that the sample size is smaller here than for the corresponding analysis used to analyse the host data. There was no significant effect of parasite diversity on PEV2 evolutionary rate (ANOVA  $F_{2,9} = 14910$ ,  $P = 0.44$ ).

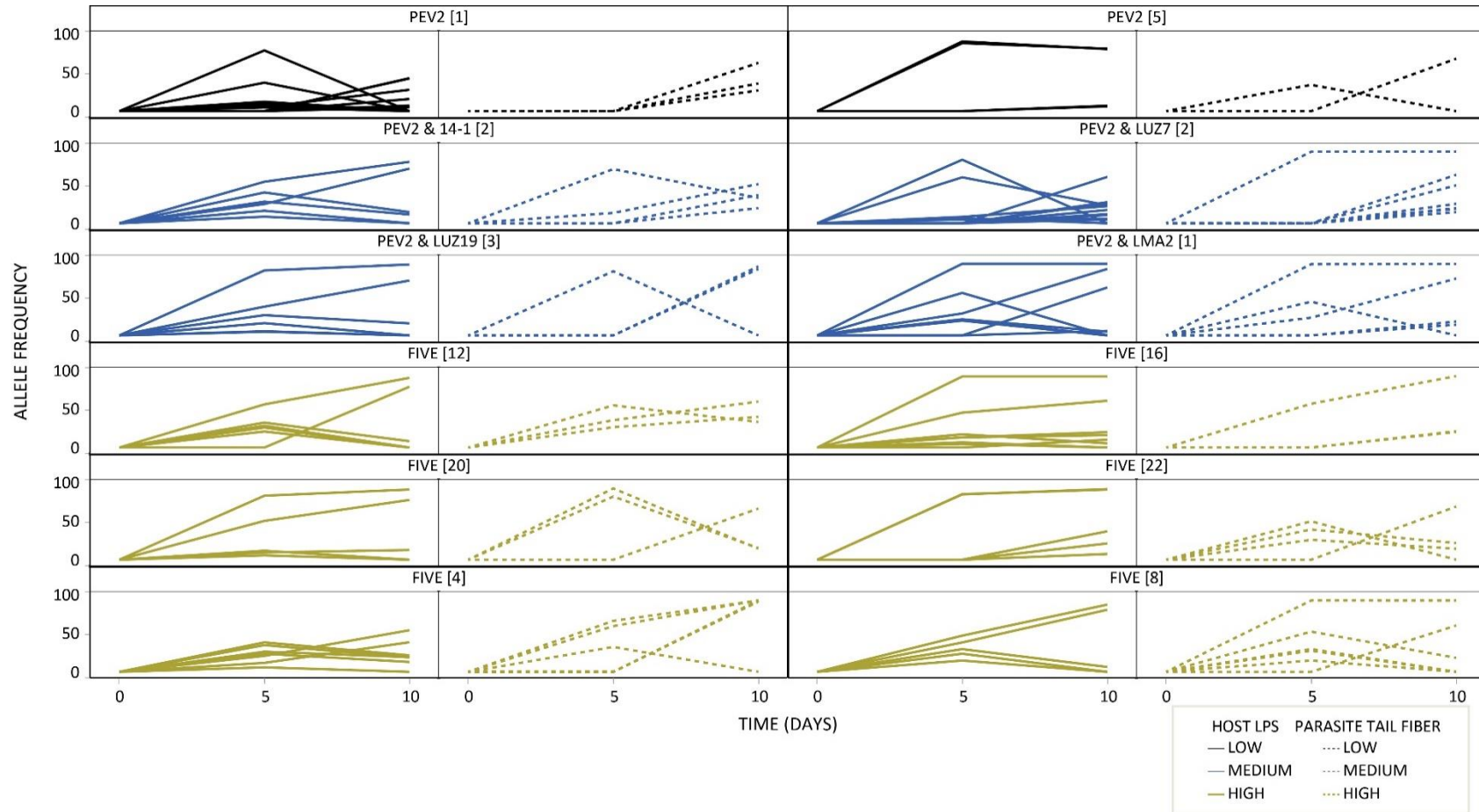


Fig. S6 Genomic evidence for antagonistic coevolution. This figure shows the host LPS biosynthesis allele frequencies (solid lines) alongside the parasite tail fiber allele frequencies (dotted lines) for the phage PEV2 across all levels of parasite diversity (low (black), medium (blue) and high (yellow)). Host LPS serves as the receptor for this parasite and the tail fibers are the means by which the parasite recognizes and binds to its receptor. These data support the phenotypic data which clearly shows increasing parasite infectivity and increasing host resistance over time and conclusively demonstrate antagonistic coevolution at the genomic level.

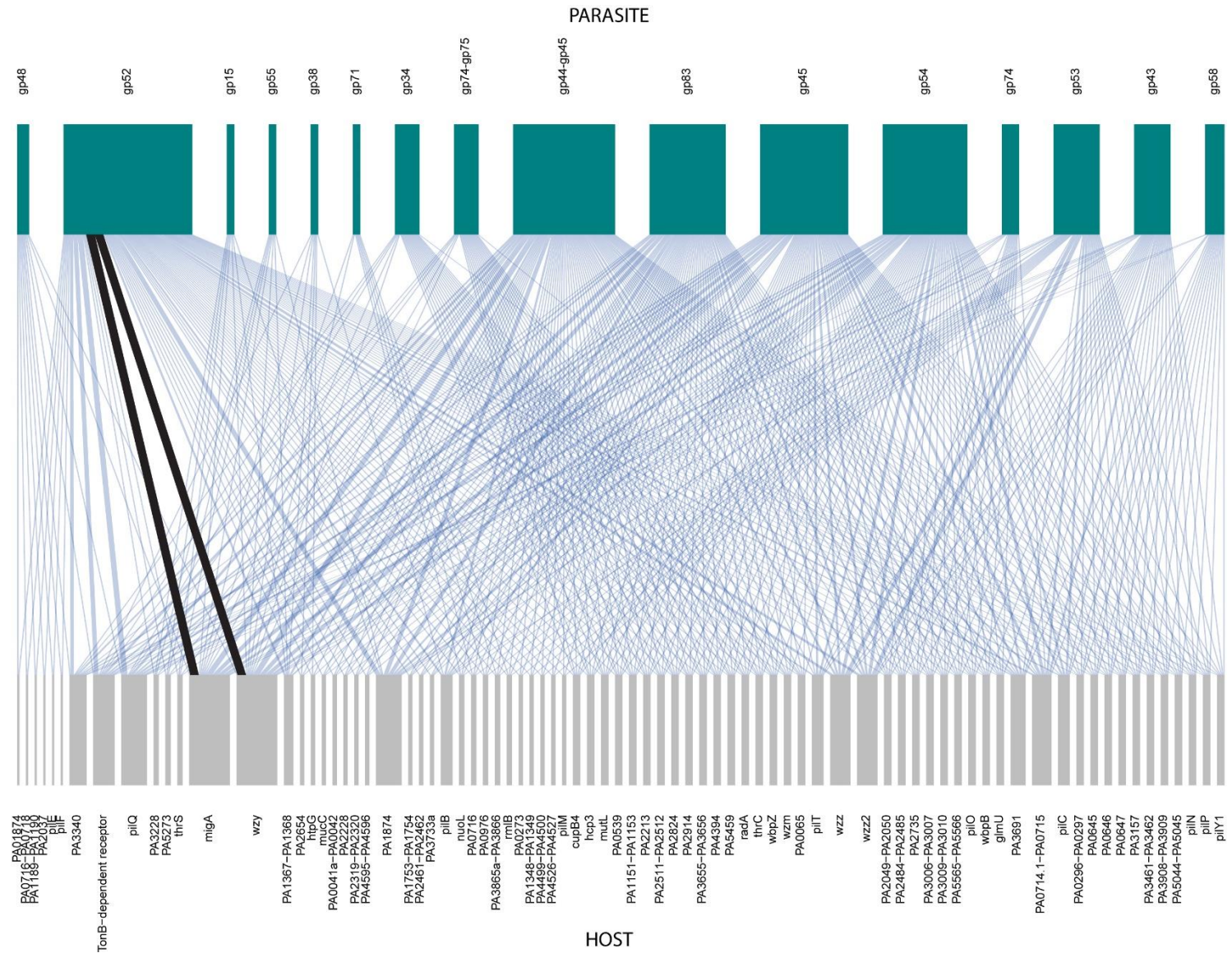


Fig. S7 Genomic evidence for genetic specificity of antagonistic coevolution. A bipartite network plot of host-parasite gene interactions across all treatments where the width of the lines is scaled by the frequency at which that interaction was observed. Previously published data has shown that host LPS genes and parasite tail fibre genes can be the focus of antagonistic coevolution (24). Using the SNP data collected for both the hosts and parasites we computed a gene interaction matrix for each of the subsampled replicates containing PEV2. For every possible host gene – parasite gene combination, we calculated the number of communities in which mutations in those genes co-occurred. To visualize the relationship the frequency at which a particular gene pair co-occurred was then used to weight the interactions in a host-parasite gene interaction network produced using bipartite in R showing every possible gene combination across all replicates. When the networks of all possible interactions between coevolved host and parasite genes (intergenic mutations are shown giving the upstream and downstream gene IDs separated by a hyphen) are examined, clear patterns start to emerge. Of the 508 possible pairwise combinations of host (bottom) and parasite (top) genes, 442 occur are unique and only 2 combinations occur in >50% of replicates. When the functions of these genes are examined the data show that in every sequenced community there are mutations in host LPS biosynthesis genes and parasite tail fibers, and by far the most common of these associations was between the host LPS biosynthesis genes (*wzy* and *migA*) and the parasite tail fiber protein gene (*gp52*) which each co-occurred in 8/12 replicates. These interactions are shown in black on the figure. The extreme overrepresentation of these associations supports previously findings in bacteriophage – host coevolution driven by mutations in host LPS biosynthesis genes and parasite tail fibers genes.



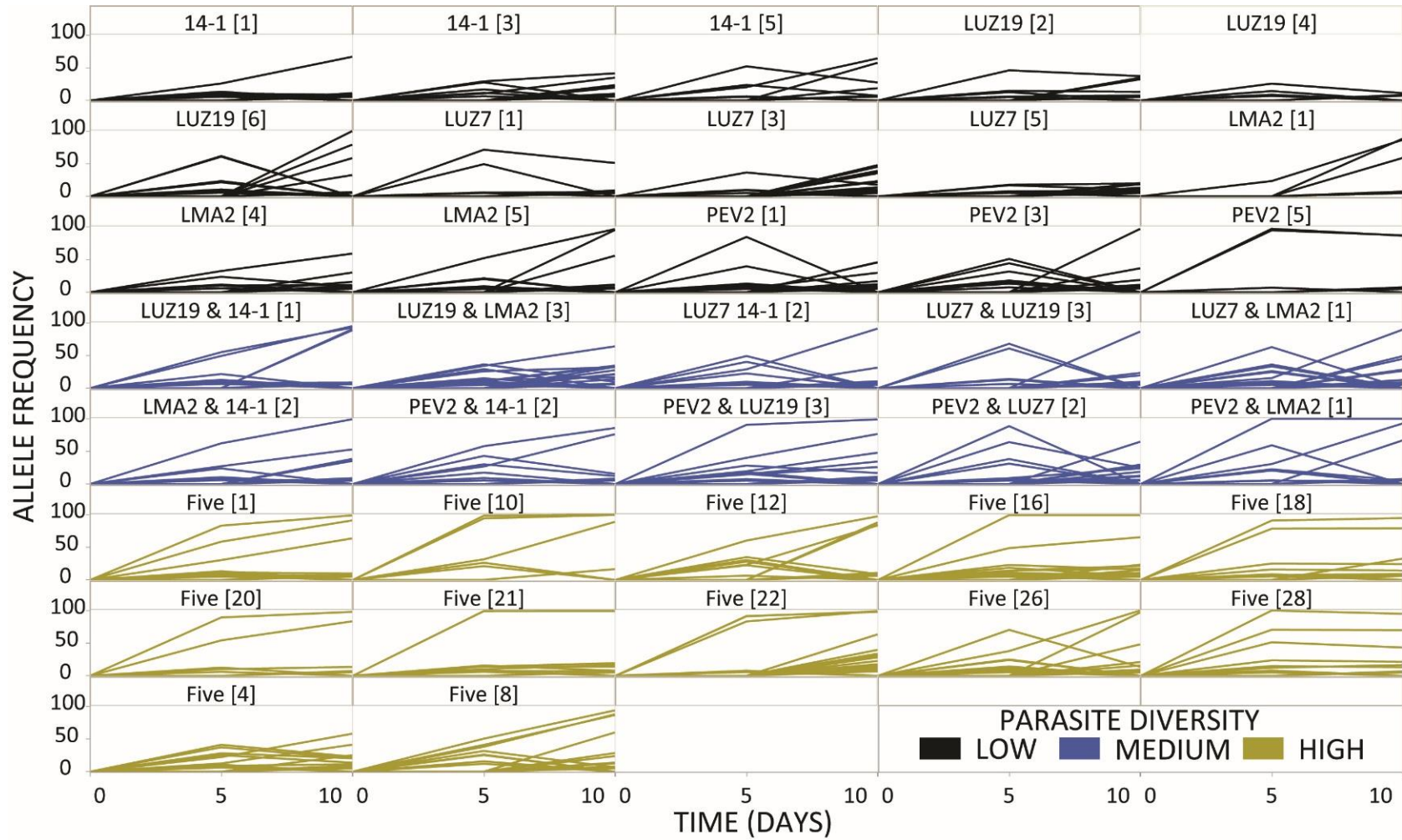


Fig. S8 Parasite diversity encourages harder selective sweeps. The frequency of each observed mutation in each sequenced population from the start, mid and endpoints of the experiments from the low (black), medium (blue) and high (yellow) parasite diversity populations. More alleles reach higher frequencies in the high parasite diversity treatment than in the medium or low.

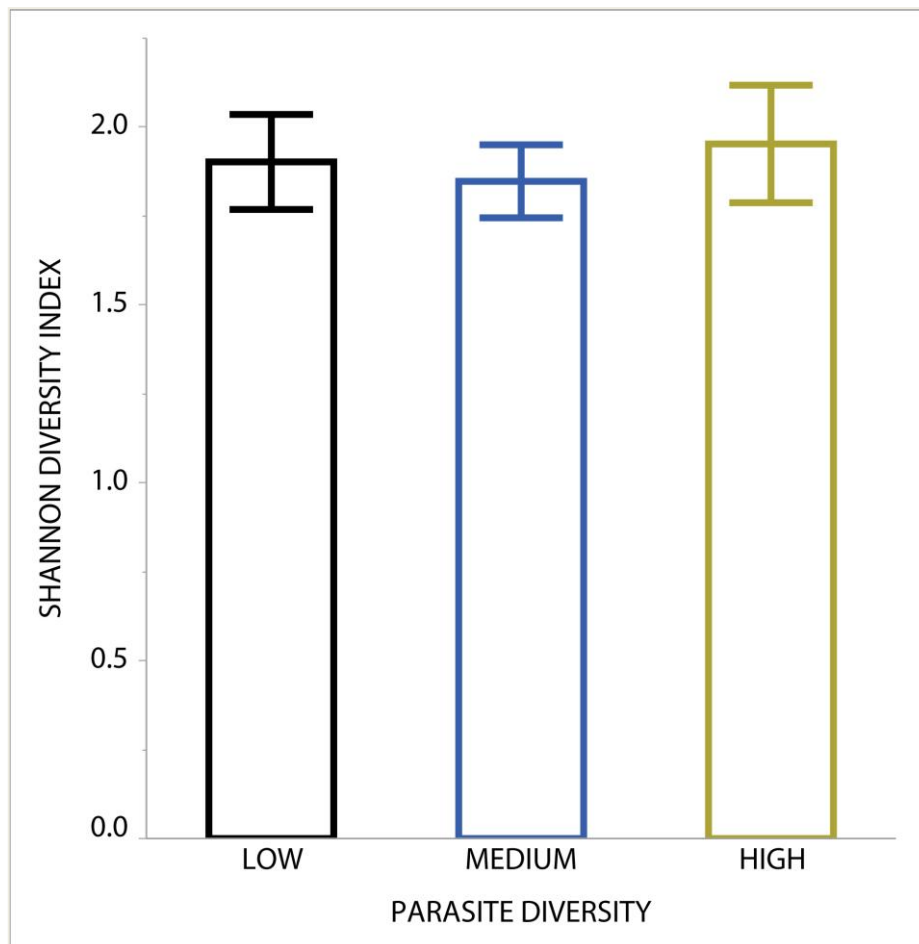


Fig. S9 Parasite diversity does not impact within sample host diversity. Shows the mean within sample diversity as scored on the Shannon Diversity index from SNP frequency data from the low (black), medium (blue) and high (yellow) parasite diversity populations. There was no significant effect of parasite diversity on within sample host diversity (ANOVA  $F_{2,34} = 0.06$ ,  $P = 0.88$ ). Error bars show 1 standard error.

**Table S1.**

Identities of host genes in which mutations were particularly likely to be detected pooled across all treatments.

Gene Function	Number of mutations	Number of genes mutated	Genes with >10 mutations
LPS Biosynthesis	190	10	PA3154 ( <i>wzy</i> ), PA3160 ( <i>wzz</i> ), PA0938 ( <i>wzz2</i> ) and PA0705 ( <i>migA</i> )
Type IV pili formation	69	17	PA5040 ( <i>pilQ</i> ) and PA4526 ( <i>pilB</i> )
TonB-dependent receptor	55	1	PA2911
Other / unknown / intergenic	368	146	PA1874

**Table S2.**

Identities of parasite (PEV2) genes in which mutations were particularly likely to be detected pooled across all treatments. The gp71 mutations all occurred in a single sample whereas gp52 was the only gene in which mutations were detected for every sample.

Gene Function	Number of mutations	Number of genes mutated	Genes with $\geq 10$ mutations
Putative tail fiber protein	83	2	gp52
RNA polymerase	10	1	gp71
Other / unknown / intergenic	132	17	gp45, gp53, gp54, gp83 and intergenic gp44-gp45



**Table S3.**

Shows the number of mutations that reached >10% frequency in each of the five parasites across all sequenced replicates alongside the proportion of these that were non-synonymous.

Phage Type	# Observed mutations	Proportion non-synonymous
14_1	44	0.9
LMA2	6	1.0
LUZ19	158	0.7
LUZ7	52	0.8
PEV2	225	0.8

**Table S4.**

This table gives details of the phage specific primer pairs used here and the identity of their target regions.

Phage	Gene	Forward Primer	Reverse Primer
PEV2	gp53	TGCCGAAGCATTGGTCAGAT	GACTACACCGACCAGTGGTG
LUZ7	gp056	TGACCACGTACTCGGTGTTG	ACAAGCTGGGCCAGTTCTAC
LUZ19	gp40	ACCCTAGCTGGTCAAGTCCT	CACCAGAGTAGTAGGCTGCC
LMA2	gp38	TACAATCAGCAGCGCATCCA	CCGGAAGTGTCTGCCAGAT
14-1	gp45	CTTAGCAGCACGACTTGGGA	CTCCACGTCCCATTCAACA